# Perovskite Solid Solutions along the $NaNbO_3$−$SrTiO_3$ Join: Phase Transitions, Formation Enthalpies, and Implications for General Perovskite Energetics

Hongwu Xu,*[,†,§] Alexandra Navrotsky,[†] Yali Su,[‡,||] and M. Lou Balmer[‡,⊥]

*Thermochemistry Facility and NEAT ORU, University of California at Davis, Davis, California 95616, and Pacific Northwest National Laboratory, P.O. Box 999, MSIN K8-93, Battelle Boulevard, Richland, Washington 99352*

*Received December 17, 2004. Revised Manuscript Received January 27, 2005*

Perovskite solid solutions along the $NaNbO_3$−$SrTiO_3$ join have been synthesized using the sol−gel and solid-state sintering methods. XRD analysis indicates that as Sr+Ti content increases, the perovskite structure changes from the orthorhombic to tetragonal and to cubic. The enthalpies of formation from the constituent oxides ($\Delta H^\circ_{f,ox}$ and from the elements ($\Delta H^\circ_{f,el}$) have been determined by drop solution calorimetry into molten $3Na_2O{\cdot}4MoO_3$ at 974 K. The formation enthalpy $\Delta H^\circ_{f,ox}$ becomes less exothermic with increasing Sr+Ti content, suggesting a destabilization effect of the substitution, $Na^+ + Nb^{5+} \rightarrow Sr^{2+} + Ti^{4+}$ on the perovskite structure with respect to the constituent oxides. The trend of decreasing thermodynamic stability with decreasing structural distortion (relative to the ideal cubic structure) is opposite to that seen in most $ABO_3$ perovskites. We interpret this behavior in terms of the dominance of acid−base chemistry, expressed by the ionic potential ratio of B to A cation $(z/r)_B/(z/r)_A$, in determining phase stability. This approach can be applied to other perovskite systems. Moreover, the enthalpic variation with Sr+Ti content is nearly linear, and thus the enthalpies of the morphotropic transitions across the series are rather small.

## Introduction

Perovskite solid solutions in the $NaNbO_3$−$SrTiO_3$ system are of interest for both practical and fundamental reasons. $NaNbO_3$ and its related perovskites possess a unique combination of physical properties such as low density, high sound velocity, and a wide range of dielectric constants.[1−4] Thus, these materials are attractive for ferroelectric and piezoelectric applications such as actuators, attenuators, and sensors. $SrTiO_3$ has high dielectric constants and excellent stability upon changing temperature and applied voltage and thereby has been widely used in the electronic industry (e.g., as internal boundary layer (IBL) capacitors.[5]). Doping of other elements such as La and Nb into $SrTiO_3$ can drastically affect its properties. For instance, Nb doping in $SrTiO_3$ changes from an insulator to an *n*-type semiconductor, and then to a metallic conductor with increasing Nb concentration.[6,7] Conductive Nb-doped $SrTiO_3$ films may be used as electrodes that require good stability at high temperatures and in an oxidized atmosphere.[7]

Although both $NaNbO_3$- and $SrTiO_3$-based perovskites have been extensively studied and utilized, the solid solution between the two compounds has received less attention. Dielectric measurements of $Na_{1-x}Sr_xNb_{1-x}Ti_xO_3$ reveal an antiferroelectric to ferroelectric transition at $x = 0.2$.[8,9] The relaxor-type behavior when $x > 0.2$ is evidenced by an abrupt drop in the maximum temperature of dielectric permittivity ($\epsilon(T)$) and an increased broadening of the $\epsilon(T)$ maxima at the critical composition.[9] Piezoelectric studies show that the in-plane electromechanical coupling coefficients ($K_p$) of $Na_{1-x}Sr_xNb_{1-x}Ti_xO_3$ increase with increasing *x*, and, further, they are significantly higher than those for other $NaNbO_3$−$ATiO_3$ (A = Mg, Co, Ni, Mn) systems.[1] These characteristics may render $Na_{1-x}Sr_xNb_{1-x}Ti_xO_3$ perovskites unique electronic applications. Furthermore, these materials do not contain lead, making them environmentally superior to $PbTiO_3$-based systems. In addition to their electrical properties, $Na_{1-x}Sr_xNb_{1-x}Ti_xO_3$ perovskites are major components in the ceramic waste forms designed for immobilization of radioactive $^{90}Sr$.

* To whom correspondence should be addressed.
† University of California at Davis.
‡ Pacific Northwest National Laboratory.
§ Present address: Los Alamos Neutron Science Center, LANSCE-12, MS-H805, Los Alamos National Laboratory, Los Alamos, NM 87545. E-mail: hxu@lanl.gov.
|| Present address: Kronos Science Laboratories, 2222 E. Highland Ave., Phoenix, AZ 85016.
⊥ Present address: Caterpillar Inc., Technical Center, E/854, P.O. Box 1875, Peoria, IL 61656.

(1) Reznitchenko, L. A.; Dergunova, N. V.; Geguzina, G. A.; Razumovskaya, O. N.; Shilkina, L. A.; Ivanova, L. S. *Inorg. Mater.* **1997**, *33*, 1277.
(2) Reznitchenko, L. A.; Dergunova, N. V.; Geguzina, G. A.; Razumovskaya, O. N.; Shilkina, L. A.; Ivanova, L. S. *Ferroelectrics* **1998**, *214*, 241.
(3) Geguzina, G. A.; Reznitchenko, L. A.; Dergunova, N. V. *Ferroelectrics* **1998**, *214*, 261.
(4) Reznitchenko, L. A.; Turik, A. V.; Kuznetsova, E. M.; Sakhnenko, V. P. *J. Phys.: Condens. Matter* **2001**, *13*, 3875.
(5) Burn, I.; Neirman, S. *J. Mater. Sci.* **1982**, *17*, 3510.
(6) Gervais, F.; Servoin, J.-L.; Baratoff, A.; Bednorz, J. G.; Binning, G. *Phys. Rev. B* **1993**, *47*, 8187.
(7) Guo, X. G.; Chen, X. S.; Sun, Y. L.; Sun, L. Z.; Zhou, X. H.; Lu, W. *Phys. Lett. A* **2003**, *317*, 501.
(8) Glaister, R. M. *J. Am. Ceram. Soc.* **1960**, *43*, 348.
(9) Raevski, I. P.; Reznitchenko, L. A.; Malitskaya, M. A.; Shilkina, L. A.; Lisitsina, S. O.; Raevskaya, S. I.; Kuznetsova, E. M. *Ferroelectrics* **2004**, *299*, 95.

10.1021/cm047785i CCC: $30.25 
Published on Web 03/08/2005

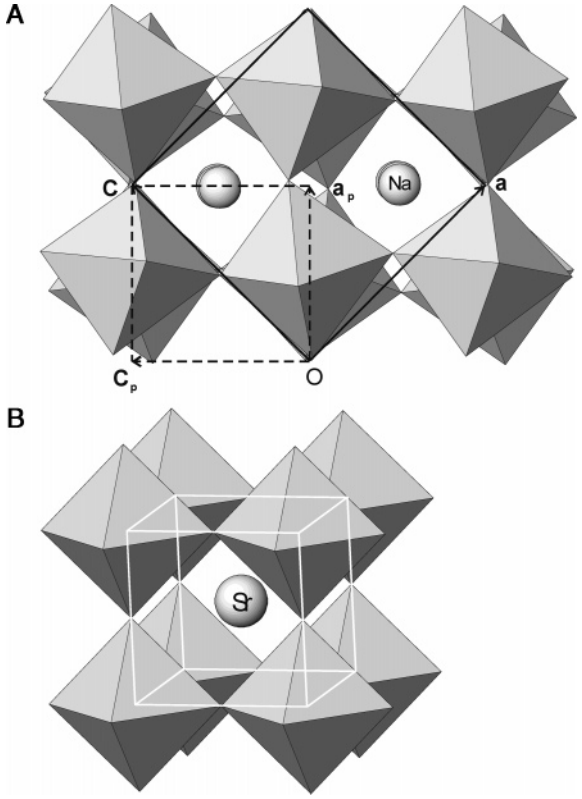


**Figure 1.** Crystal structures of (A) $NaNbO_3$ (projected down [010]) and (B) $SrTiO_3$ perovskites. Octahedra represent $[NbO_6]$ or $[TiO_6]$ units, and spheres represent $Na^+$ or $Sr^{2+}$ ions. Solid lines outline the unit cell, and dashed lines in (A) outline the pseudocubic subcell.

In particular, a recently synthesized series of octahedral microporous materials, $NaTi_xNb_{2-x}O_{6-x}(OH)_x{\cdot}H_2O$,[10−12] exhibits high selectivity for $Sr^{2+}$ over alkali cations and thus can potentially be used for extraction of $^{90}Sr$ from aqueous nuclear wastes and contaminated groundwater. Calcination of the Sr-loaded ion exchangers into a stable ceramic waste form is a proposed strategy.[10−13] These perovskite phases, which also occur in the well-known SYNROC ceramic waste form,[14] appear on calcination and are expected to have high thermal stability and chemical durability.

The $NaNbO_3$−$SrTiO_3$ series is also interesting from the viewpoint of crystal chemistry. Like other $ABO_3$ perovskites, $NaNbO_3$ and $SrTiO_3$ comprise a three-dimensional framework of corner-sharing $[BO_6]$ (B = Nb or Ti) octahedra with A cations (A = Na or Sr) occupying its cavities (Figure 1). At room temperature, $SrTiO_3$ possesses the ideal, cubic perovskite structure (space group $Pm\bar{3}m$) in which the bond angle Ti−O−Ti = 180° (Figure 1B). Upon cooling, it transforms to a tetragonal phase (space group $P4_2/nbm$) at 110 K.[15] In contrast, the room-temperature structure of $NaNbO_3$ is orthorhombic (space group *Pbma* or *Pbcm*) (Figure 1A)[16,17] or even monoclinic.[18] On heating, $NaNbO_3$ undergoes one of the most complicated sequences of displacive transitions to phases with higher symmetries and eventually becomes cubic at ∼914 K.[19−22] On cooling, it converts to the rhombohedral phase (*R*3*c*) at ∼163 K.[23] These transitions occur largely via tilting of $[NbO_6]$ or $[TiO_6]$ octahedra about the cubic or pseudocubic ⟨100⟩ axes. In particular, with increasing temperature, the tilting angles in $NaNbO_3$ gradually decrease and become zero at ∼914 K, where the cubic phase forms. Since $SrTiO_3$ possesses the ideal cubic structure at room temperature, one expects that the $NaNbO_3$−$SrTiO_3$ series may undergo a similar sequence of transitions with increasing Sr+Ti content. Thus, the $Na^+ + Nb^{5+} \rightarrow Sr^{2+} + Ti^{4+}$ substitution may mimic temperature in its effects on the $NaNbO_3$ perovskite framework.

Despite the extensive interests in $NaNbO_3$−$SrTiO_3$ perovskites, little is known about their thermodynamics and its relation to the crystal chemistry. Thermochemical data, including the enthalpies of formation, of these phases are essential to assess and predict their stability and their compatibility with other components at application conditions. In this study, a suite of $Na_{1-x}Sr_xNb_{1-x}Ti_xO_3$ perovskites was synthesized using the sol−gel and solid-sate sintering methods. Unit-cell parameters of perovskites having different symmetries have been determined by Rietveld analysis of powder X-ray diffraction (XRD) data. Differential scanning calorimetry (DSC) was performed to examine their thermally induced phase transitions. The enthalpies of formation from the constituent oxides and from the elements have been measured using high-temperature drop solution calorimetry into molten $3Na_2O{\cdot}4MoO_3$ at 974 K. Trends in the formation enthalpies of $Na_{1-x}Sr_xNb_{1-x}Ti_xO_3$ are related to the ionic potential ratio $(z/r)_B/(z/r)_A$ (A = Na, Sr; B = Nb, Ti). Implications for the general energetics of $ABO_3$ perovskites are discussed.

## Experimental Methods

**Sample Synthesis.** Five samples with the compositions $Na_{1-x}Sr_xNb_{1-x}Ti_xO_3$, $x$ = 0, 0.25, 0.5, 0.75, and 1, were used in this study. $NaNbO_3$ was prepared using a sol−gel processing route, $SrTiO_3$ purchased from Alfa Aesar (99.999%), and the intermediate phases synthesized by high-temperature solid-state sintering. $NaNbO_3$ was synthesized as follows. First, an amorphous, homogeneous precursor was prepared using niobium ethoxide (NbEO) and sodium hydroxide. An appropriate amount of NbEO was weighed and poured in a reaction flask in a glovebox under Ar atmosphere, and the flask was sealed with a rubber stopper and transferred to a stir plate. A solution of NaOH (50 wt %) and ethanol

(10) Nyman, M.; Tripathi, A.; Parise, J. B.; Maxwell, R. S.; Harrison, W. T. A.; Nenoff, T. M. *J. Am. Chem. Soc.* **2001**, *123*, 1529.
(11) Nyman, M.; Tripathi, A.; Parise, J. B.; Maxwell, R. S.; Nenoff, T. M. *J. Am. Chem. Soc.* **2002**, *124*, 1704.
(12) Xu, H.; Nyman, M.; Nenoff, T. M.; Navrotsky, A. *Chem. Mater*. **2004**, *16*, 2034.
(13) Su, Y.; Balmer, M. L.; Wang, L.; Bunker, B. C.; Nyman, M.; Nenoff, T.; Navrotsky, A. In *Scientific Basis for Nuclear Waste Management XXII*; Wronkiewicz, D. J., Lee, J. H., Eds.; Mater. Res. Soc. Symp. Proc. 556; Materials Research Society: Pittsburgh, PA, 1999; pp 77−84.
(14) Ringwood, A. E.; Kesson, S. E.; Ware, N. G.; Hibberson, W.; Major, A. *Nature* **1979**, *278*, 219.
(15) Fleury, P. A.; Scott, J. F.; Worlock, J. M. *Phys. Rev. Lett.* **1968**, *21*, 16.
(16) Sakowski-Cowley, A. C.; Lukaszewicz, K.; Megaw, H. D. *Acta Crystallogr.* **1969**, *B25*, 851.
(17) Hewat, A. W. *Ferroelectrics* **1974**, *7*, 83.
(18) Darlington, C. N. W.; Knight, K. S. *Physica* **1999**, *B266*, 368.
(19) Ahtee, M.; Glazer, A. M.; Megaw, H. D. *Philos. Mag.* **1972**, *26*, 995.
(20) Glazer, A. M.; Megaw, H. D. *Philos. Mag.* **1972**, *25*, 1119.
(21) Darlington, C. N. W.; Knight, K. S. *Acta Crystallogr.* **1999**, *B55*, 24.
(22) Glazer, A. M.; Megaw, H. D. *Acta Crystallogr.* **1973**, *A29*, 489.
(23) Darlington, C. N. W.; Megaw, H. D. *Acta Crystallogr.* **1973**, *B29*, 2171.

**Table 1. Chemical Compositions of $NaNbO_3-SrTiO_3$ Perovskite Samples**

| nominal composition | measured composition[a] |
|---|---|
| $75\%NaNbO_3-25\%SrTiO_3$ | $Na_{0.72}Nb_{0.76}Sr_{0.24}Ti_{0.25}O_3$ |
| $50\%NaNbO_3-50\%SrTiO_3$ | $Na_{0.48}Nb_{0.50}Sr_{0.49}Ti_{0.51}O_3$ |
| $25\%NaNbO_3-75\%SrTiO_3$ | $Na_{0.22}Nb_{0.26}Sr_{0.74}Ti_{0.75}O_3$ |

[a] Errors are in the range of 0.01−0.02.

was then injected into the flask containing NbEO using a syringe, followed by the injection of an equal volume of ethanol. This process was repeated several times with intervals of 15 min until the ratio Na:Nb = 1:1. After gelation, additional water and ethanol were added to dissolve the gel, and the liquid was then stirred and dried in air overnight. Second, ~0.5 g of the obtained precursor was ground, pressed into pellets, and then heat-treated in air at 1173 K for ~15 h.

The $Na_{1-x}Sr_xNb_{1-x}Ti_xO_3$ phases with $x = 0.25$, 0.5, and 0.75 were synthesized from reagent-grade chemicals $Na_2CO_3$, $SrCO_3$, $Nb_2O_5$, and $TiO_2$ through solid-state reaction. The reactants in desired ratios were mixed, dried, pressed into pellets, and heated at 1123 K for ~12 h. After the initial cycle, the pellets were ground and reheated at the same conditions once or twice to achieve complete reaction. The final products were white, monophasic, and well-crystallized materials (see below).

**Sample Characterization.** *Electron Microprobe Analysis.* Chemical compositions of the synthesized samples were confirmed by electron probe microanalysis using a Cameca SX-50 microprobe operated at 20 keV and 10 nA. The calibration standards used were as follows: $NaAlSi_3O_8$ feldspar (albite) for $Na_2O$, $SrTiO_3$ perovskite for SrO, $Nb_2O_5$ crystal for $Nb_2O_5$, and rutile for $TiO_2$. The measured compositions are in good agreement with the targeted values (Table 1). The slightly lower Na contents may result from migration or evaporation of $Na^+$ under electron irradiation, a problem commonly encountered with microprobe analysis. Thus, for the later discussions, the nominal sample compositions will be used. In addition, energy-dispersive spectroscopy (EDS) mapping and back-scattered electron (BSE) imaging revealed that all the samples are homogeneous and phase-pure.

*Powder X-ray Diffraction.* Powder XRD experiments were conducted with a Scintag Pad-V diffractometer using Cu Kα radiation. Sample powders were mounted in a front-loading, shallow-cavity zero-background quartz holder, and data were collected from 5° to 120° $2\theta$ in step scan mode using steps of 0.02° with a counting time of 10 s.

To determine unit-cell parameters, the X-ray data were analyzed with the GSAS program.[24] The starting structural parameters for $Na_{1-x}Sr_xNb_{1-x}Ti_xO_3$ are from the following studies: Sakowski-Cowley et al.[16] for $x = 0$; Chung and Kim[25,26] for $x = 0.25$ and 0.5; and Megaw[27] for $x = 0.75$ and 1. Backgrounds were modeled with a shifted Chebyshev function and peak profiles fitted to pseudo-Voigt convolution functions with corrections in peak asymmetry and specimen displacement.

**Calorimetry.** *Differential Scanning Calorimetry.* To examine the phase transition behavior at elevated temperatures, differential scanning calorimetry was carried out using a Netzsch 404 or 449 high-temperature calorimeter. About 50 mg of sample powders was tightly packed in a Pt crucible before loading into the calorimeter.

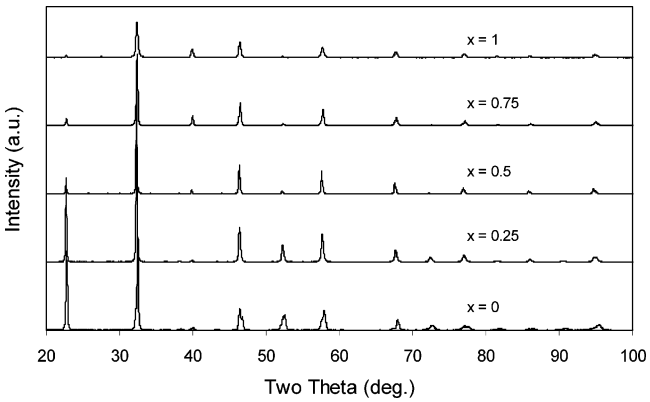


**Figure 2.** Powder X-ray diffraction patterns of $Na_{1-x}Sr_xNb_{1-x}Ti_xO_3$ perovskites with $x = 0$, 0.25, 0.5, 0.75, and 1.

Continuous scans of the baseline (empty Pt crucible), standard (sapphire), and sample were run at a scan rate of 10 K/min up to 1073 K in a flowing Ar atmosphere. Heat capacities (and thus enthalpies of transition) of the sample were calculated by applying the calibration curve, obtained from the sapphire data and the known heat capacity values of α-$Al_2O_3$, to the sample measurement.

*High-Temperature Drop-Solution Calorimetry.* High-temperature calorimetric measurements were performed using a custom-built Tian-Calvet microcalorimeter operating at 974 K with molten sodium molybdate ($3Na_2O{\cdot}4MoO_3$) as the solvent. The equipment and experimental procedure have been described in detail by Navrotsky.[28] A sample pellet weighing ~5 mg was dropped from room temperature into the solvent in the hot calorimeter. The heat effect measured includes the energy associated with heating the sample from room temperature to 974 K (heat content) plus the enthalpy of solution of the sample. The calorimeter was calibrated against the known heat content of ~5 mg corundum pellets. Between six and twelve sample pellets were dropped for each composition. To ensure there is no surface water, which would have a significant endothermic effect, present in samples, all the samples were dried at ~403 K overnight immediately before the calorimetric experiments. A drop solution experiment of $SrCO_3$ (Alfa Aesar 99.994%) was carried out under a flowing Ar atmosphere with a flow rate of ~90 $cm^3$/min to sweep out the evolved $CO_2$.[29] This measurement provided reference data for SrO for the enthalpy of formation calculations. All other experiments were performed in static air.

## Results and Discussion

**Unit-Cell Parameters and Morphotropic Transitions.** All the XRD patterns of $Na_{1-x}Sr_xNb_{1-x}Ti_xO_3$ phases can be indexed in terms of the basic perovskite structure. However, with increasing Sr+Ti content, certain sets of split diffraction peaks in $NaNbO_3$ are gradually converged and eventually merged into single peaks, suggesting a systematic increase in crystal symmetry (Figure 2). As described earlier, the ambient temperature structure of $NaNbO_3$ is orthorhombic (space group *Pbma* or *Pbcm*, though a recent neutron diffraction study argues that it may be monoclinic.[18]), whereas that of $SrTiO_3$ is cubic ($Pm\bar{3}m$). Thus, one expects that the $NaNbO_3-SrTiO_3$ solid solutions adopt the intermediate structures between the two end-members. Chung and Kim

(24) Larson A. C.; Von Dreele, R. B. *GSAS − General Structure Analysis System*; Los Alamos National Laboratory Report No. LAUR 86-748; Los Alamos National Laboratory: Los Alamos, NM, 2000.
(25) Chung, H.-T.; Kim, H.-G. *Han'guk Chaelyo Hakhoechi* **1995**, *5*, 748 (cited in the Inorganic Crystal Structure Database, 2003).
(26) Chung, H.-T.; Kim, H.-G. *Yoop Hakoechi* **1995**, *32*, 582 (cited in the Inorganic Crystal Structure Database, 2003).
(27) Megaw, H. D. *J. Inorg. Nucl. Chem.* **1960**, *15*, 356.
(28) Navrotsky, A. *Phys. Chem. Miner.* **1997**, *24*, 222.
(29) Navrotsky, A.; Rapp, R. P.; Smelik, E.; Burnly, P.; Circone, S.; Chai, L.; Bose, K.; Westrich, H. R. *Am. Mineral.* **1994**, *79*, 1099.

**Table 2. Unit-Cell Parameters of $Na_{1-x}Sr_xNb_{1-x}Ti_xO_3$ Perovskites**

| $x$ | symmetry | $a$ (Å) | $b$ (Å) | $c$ (Å) | $V$ (Å$^3$) | $V_p$ (Å$^3$)[a] |
|---|---|---|---|---|---|---|
| 0 | orthorhombic | 5.5625(4) | 15.5495(10) | 5.5138(4) | 476.91(8) | 59.614(9) |
| 0.25 | orthorhombic | 5.5387(1) | 7.8271(2) | 5.5494(2) | 240.58(1) | 60.145(3) |
| 0.5 | tetragonal | 5.5405(1) | | 7.8504(2) | 240.99(1) | 60.248(3) |
| 0.75 | cubic | 3.9129(1) | | | 59.910(4) | 59.910(4) |
| 1 | cubic | 3.9150(1) | | | 60.007(5) | 60.007(5) |

[a] Unit-cell volume of the pseudocubic or cubic cell.

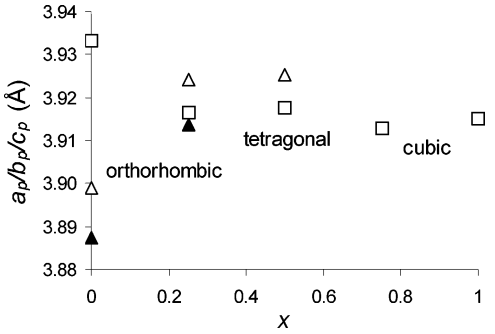


**Figure 3.** Variation of cell parameters in terms of the pseudocubic subcell for $Na_{1-x}Sr_xNb_{1-x}Ti_xO_3$ perovskites as a function of composition. Squares, solid triangles, and empty triangles represent $a_p$, $b_p$, and $c_p$, respectively. Errors are smaller than the size of symbols.

synthesized two intermediate phases, $Na_{0.7}Sr_{0.3}Nb_{0.7}Ti_{0.3}O_3$ and $Na_{0.3}Sr_{0.7}Nb_{0.3}Ti_{0.7}O_3$, and determined their symmetries to be orthorhombic (*Pnma*) and tetragonal (*I*4/*mmm*), respectively.[25,26] Unit-cell analysis of our intermediate samples with $x = 0.25$, 0.5, and 0.75 indicates that they are orthorhombic, tetragonal, and cubic, respectively. In other words, as Si+Ti content increases, a series of morphotropic phase transitions occur. These compositionally induced transitions may be analogous to the transformations in $NaNbO_3$ on heating (orthorhombic → tetragonal → cubic) and in $SrTiO_3$ on cooling (cubic → tetragonal). However, to determine the critical compositions (or if two-phase regions exist) and the character of the morphotropic transitions, more compositions across the series need to be studied.

Unit-cell parameters of $Na_{1-x}Sr_xNb_{1-x}Ti_xO_3$ determined by Rietveld analysis are presented in Table 2 and Figure 3. For ease of comparison, cell parameters ($a$, $b$, and $c$) are plotted in terms of the pseudocubic subcell parameters ($a_p$, $b_p$, $c_p$) (Figure 3). With increasing Sr+Ti content, $a_p$, $b_p$, and $c_p$ for the orthorhombic structure become closer, then two of them become identical (tetragonal) at $x = 0.5$, and finally all the parameters are equal (cubic) at $x \geq 0.75$. This behavior is consistent with the morphotropic transitions described above and can be explained in terms of the tolerance factor ($t$) for $ABO_3$ perovskites: $t = (r_A + r_O)/\sqrt{2}(r_B + r_O)$, where $r_A$, $r_B$, and $r_O$ refer to the ionic radius of A, B, and $O^{2-}$, respectively. In the ideal cubic perovskite structure, the ratio of the A−O bond length ($r_A + r_O$) to the B−O length ($r_B + r_O$) equals $\sqrt{2}$, and thus $t = 1$. When this condition cannot be met, the structure distorts, largely via tilting of its [$BO_6$] octahedra, and thereby departs from the cubic symmetry.[30] In orthorhombic $NaNbO_3$ ($t \approx 0.94$), the Nb−O bond is longer than needed to match the Na−O bond to form an ideal cubic structure. With increasing $Na^+ + Nb^{5+} \rightarrow Sr^{2+} + Ti^{4+}$ substitution, however, the mean bond length ⟨B−O⟩ (B = Nb, Ti) decreases, whereas ⟨A−O⟩ (A = Na, Sr) increases, resulting in the tolerance factor $t$ approaching unity. In other words, the perovskite structure changes systematically toward the cubic symmetry of the end-member $SrTiO_3$ ($t \approx 1$).

**Table 3. Enthalpies of Drop Solution in Sodium Molybdate at 974 K and Enthalpies of Formation from the Oxides and from the Elements at 298 K for $Na_{1-x}Sr_xNb_{1-x}Ti_xO_3$ Perovskites**

| x | $\Delta H_{ds}$ (kJ/mol)[a] | $\Delta H^\circ_{f,ox}$ (kJ/mol) | $\Delta H^\circ_{f,el}$ (kJ/mol) |
|---|---|---|---|
| 0 | 94.6 ± 0.5 (12) | −157.4 ± 2.2 | −1314.6 ± 3.1 |
| 0.25 | 83.1 ± 0.7 (6) | −148.4 ± 1.8 | −1399.9 ± 2.4 |
| 0.5 | 72.3 ± 0.9 (8) | −140.0 ± 1.8 | −1485.9 ± 2.1 |
| 0.75 | 60.6 ± 0.9 (6) | −130.8 ± 1.9 | −1571.0 ± 2.2 |
| 1 | 44.4 ± 0.3 (6) | −117.1 ± 2.1 | −1651.6 ± 2.4 |

[a] Uncertainty is two standard deviations of the mean; value in ( ) is the number of experiments.

Although the structures of $Na_{1-x}Sr_xNb_{1-x}Ti_xO_3$ vary with composition, unit-cell volume remains largely unchanged across the series (Table 2). Apparently, the volume expansion due to the substitution of $Na^+$ ($r_{Na} = 1.18$ Å in 8-coordination[31]) by the larger $Sr^{2+}$ ($r_{Sr} = 1.44$ Å in 12-coordination[31]) approximately cancels out the contraction due to the replacement of $Nb^{5+}$ ($r_{Nb} = 0.64$ Å in 6-coordination[31]) by the smaller $Ti^{4+}$ (0.605 Å in 6-coordination[31]). As commonly occurs in other solid solutions, the intermediate $Na_{1-x}Sr_xNb_{1-x}Ti_xO_3$ phases may have some degrees of Na/Sr and/or Nb/Ti short-range order, which can affect the volume. However, the slight volume variations coupled with the multiple morphotropic transitions in this series do not allow extraction of the detailed mixed-cation order−disorder information.

**Enthalpies of Formation.** The measured heats of drop solution ($\Delta H_{ds}$) of $Na_{1-x}Sr_xNb_{1-x}Ti_xO_3$ perovskites in molten $3Na_2O{\cdot}4MoO_3$ at 974 K are presented in Table 3. For calculations of the standard molar enthalpies of formation, the heats of drop solution of the constituent oxides are needed (Table 4). The $\Delta H_{ds}$ values of $Na_2O$, $Nb_2O_5$, and $TiO_2$ are taken from the literature;[32−34] that of SrO was derived from our own drop-solution experiment of $SrCO_3$ through the thermodynamic cycle listed in Table 5. Because of the hygroscopic nature of SrO, the $\Delta H_{ds}$ of $SrCO_3$ was measured instead. The derived $\Delta H_{ds}$ of SrO (−131.4 ± 1.9 kJ/mol) isin agreement with that from an earlier study (−135.8 ± 2.5 kJ/mol[37]) within the experimental error.

Using the $\Delta H_{ds}$ data for $Na_{1-x}Sr_xNb_{1-x}Ti_xO_3$ and the constituent oxides, we calculated the standard molar enthal-

(30) Navrotsky, A. *Chem. Mater.* **1998**, *10*, 2787.
(31) Shannon, R. D. *Acta Crystallogr.* **1976**, *A32*, 751.
(32) Tessier, F.; Navrotsky, A.; Le Sauze, A.; Marchand, R. *Chem. Mater.* **2000**, *12*, 148.
(33) Pozdnyakova, I.; Navrotsky, A.; Shilkina, L.; Reznichenko, L. *J. Am. Ceram. Soc.* **2002**, *85*, 379.
(34) Putnam, R. L.; Navrotsky, A.; Woodfield, B. F.; Boerio-Goates, J.; Shapiro, J. L. *J. Chem. Thermodyn.* **1999**, *31*, 229.

**Table 4. Enthalpies of Drop Solution in Sodium Molybdate at 974 K and Enthalpies of Formation from the Elements at 298 K of Several Oxides Used in Calculations of the Enthalpies of Formation of $Na_{1-x}Sr_xNb_{1-x}Ti_xO_3$ Perovskites**

| oxide | $Na_2O$ | SrO | $Nb_2O_5$ | $TiO_2$ |
|---|---|---|---|---|
| $\Delta H_{ds}$ (kJ/mol) | $-217.56 \pm 4.25$[a] | $-131.42 \pm 1.89$[b] | $91.97 \pm 0.78$[c] | $58.73 \pm 0.91$[d] |
| $\Delta H^\circ_{f,el}$ (kJ/mol) | $-414.8 \pm 0.3$[e] | $-590.5 \pm 0.9$[e] | $-1899.54 \pm 4.2$[f] | $-944.0 \pm 0.8$[e] |

[a] From ref 32. [b] This study. [c] From ref 33. [d] From ref 34. [e] From ref 35. [f] From ref 36.

**Table 5. Thermochemical Cycle Used for Calculation of the Enthalpy of Drop Solution of SrO in Sodium Molybdate at 974 K**

| | |
|---|---|
| $SrCO_3$ (s, 298 K) → SrO (soln, 974 K) + $CO_2$ (g, 974 K)<br>$\Delta H_1 = 134.48 \pm 0.58$ kJ/mol[a] | (1) |
| SrO (s, 298 K) + $CO_2$ (g, 298 K) → $SrCO_3$ (s, 298 K)<br>$\Delta H_2 = -233.9 \pm 1.8$ kJ/mol[b] | (2) |
| $CO_2$ (g, 974 K) → $CO_2$ (g, 298 K)<br>$\Delta H_3 = -32.0$ kJ/mol[b] | (3) |
| SrO (s, 298 K) → SrO (soln, 974 K)<br>$\Delta H_4 = \Sigma \Delta H_i$ ($i = 1-3$) | (4) |

[a] This study. [b] From ref 35.

pies of formation of the perovskites from the constituent oxides ($\Delta H^\circ_{f,ox}$) via the thermochemical cycle shown in Table 6. Similarly, the enthalpies of formation from the elements ($\Delta H^\circ_{f,el}$) can be derived from their $\Delta H^\circ_{f,ox}$ values and the $\Delta H^\circ_{f,el}$ values of the constituent oxides (Table 4) by using an appropriate reaction cycle (Table 6). The enthalpies of formation thus obtained are presented in Table 3. The only previously reported enthalpies of formation at 298 K in this system are for the end-member $NaNbO_3$ ($\Delta H^\circ_{f,ox} = -153.5 \pm 2.3$ kJ/mol; $\Delta H^\circ_{f,el} = -1312.2 \pm 3.8$ kJ/mol),[33] and they are in good agreement with our values ($\Delta H^\circ_{f,ox} = -157.4 \pm 2.2$ kJ/mol; $\Delta H^\circ_{f,el} = -1314.6 \pm 3.1$ kJ/mol). Figure 4A shows the enthalpies of formation of $Na_{1-x}Sr_xNb_{1-x}Ti_xO_3$ perovskites from the oxides as a function of composition. As Sr+Ti content increases, $\Delta H^\circ_{f,ox}$ becomes less exothermic. This behavior suggests a destabilizing effect of the charge-coupled substitution, $Na^+ + Nb^{5+} \rightarrow Sr^{2+} + Ti^{4+}$, on the perovskite structure with respect to the constituent oxides.

**Energetic Systematics.** As described earlier, with increasing Sr+Ti content, the tolerance factor $t$ of $Na_{1-x}Sr_xNb_{1-x}Ti_xO_3$ approaches unity. Thus, the framework distortion of the perovskites relative to the ideal cubic structure decreases. The trend of less exothermic in $\Delta H^\circ_{f,ox}$ with increasing Sr+Ti content (Figure 4A) means that the less the structure deviates from the cubic symmetry, the less stable the $Na_{1-x}Sr_xNb_{1-x}Ti_xO_3$ perovskites are with respect to their constituent oxides (Figure 4B). However, previous thermochemical studies demonstrate that most perovskites display the opposite trend; i.e., the smaller the $(1 - t)$, the more negative the $\Delta H^\circ_{f,ox}$.[38] Only recently, two series of oxygen-deficient perovskites, $NaNb_{1-x}Ti_xO_{3-0.5x}$[39] and Mg/Sr/Ba-doped $LaGaO_3$,[40] were reported to exhibit stability relation inconsistent with this general trend. Since $Na_{1-x}Sr_xNb_{1-x}Ti_xO_3$ perovskites have full occupancies on their oxygen sublattice,

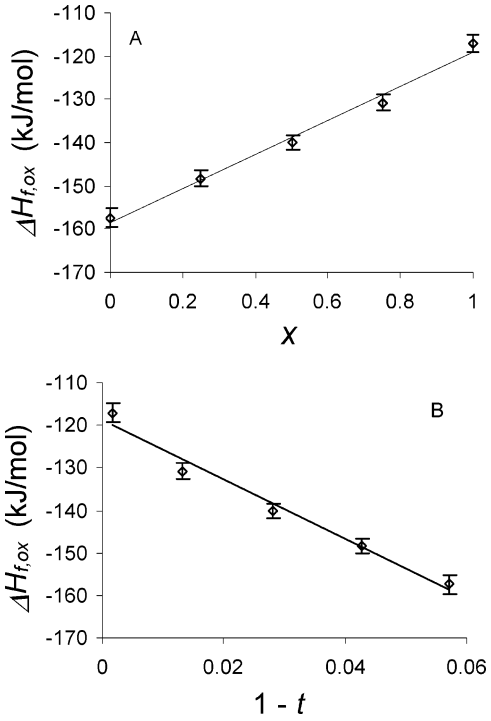


**Figure 4.** Variation of the enthalpies of formation of $Na_{1-x}Sr_xNb_{1-x}Ti_xO_3$ perovskites from the oxides at 298 K as a function of (A) $x$ and (B) $(1 - t)$. The lines are the best fits to the data.

they represent the first reported general perovskite series

**Table 6. Thermochemical Cycles Used for Calculations of the Standard Enthalpies of Formation of $Na_{1-x}Sr_xNb_{1-x}Ti_xO_3$ Perovskites**

| | | |
|---|---|---|
| Enthalpy of Formation of $Na_{1-x}Sr_xNb_{1-x}Ti_xO_3$ from the Oxides at 298 K | | |
| $[(1-x)/2]Na_2O$ (s, 298 K) → $[(1-x)/2]Na_2O$ (soln, 974 K) | (5) | $\Delta H_5$ |
| $x$SrO (s, 298 K) → $x$SrO (soln, 974 K) | (6) | $\Delta H_6$ |
| $[(1-x)/2]Nb_2O_5$ (s, 298 K) → $[(1-x)/2]Nb_2O_5$ (soln, 974 K) | (7) | $\Delta H_7$ |
| $x TiO_2$ (s, 298 K) → $x TiO_2$ (soln, 974 K) | (8) | $\Delta H_8$ |
| $[(1-x)/2]Na_2O$ (soln, 974 K) + $x$SrO (soln, 974 K) + $[(1-x)/2]Nb_2O_5$ (soln, 974 K) + $x TiO_2$ (soln, 974 K) → $Na_{1-x}Sr_xNb_{1-x}Ti_xO_3$ (s, 298 K) | (9) | $\Delta H_9$ |
| $[(1-x)/2]Na_2O$ (s, 298 K) + $x$SrO (s, 298 K) + $[(1-x)/2]Nb_2O_5$ (s, 298 K) + $x TiO_2$ (s,z 298 K) → $Na_{1-x}Sr_xNb_{1-x}Ti_xO_3$ (s, 298 K)<br>$\Delta H^\circ_{f,ox} = \Sigma \Delta H_i$ ($i = 5-9$) | (10) | |
| Enthalpy of Formation of $Na_{1-x}Sr_xNb_{1-x}Ti_xO_3$ from the Elements at 298 K | | |
| $(1-x)$Na (s, 298 K) + $[(1-x)/4]O_2$ (g, 298 K) → $[(1-x)/2]Na_2O$ (s, 298 K) | (11) | $\Delta H_{11}$ |
| $x$Sr (s, 298 K) + $(x/2)O_2$ (g, 298 K) → $x$SrO (s, 298 K) | (12) | $\Delta H_{12}$ |
| $(1-x)$Nb (s, 298 K) + $[(5-5x)/4]O_2$ (g, 298 K) → $[(1-x)/2]Nb_2O_5$ (s, 298 K) | (13) | $\Delta H_{13}$ |
| $x$Ti (s, 298 K) + $xO_2$ (g, 298 K) → $x TiO_2$ (s, 298 K) | (14) | $\Delta H_{14}$ |
| $[(1-x)/2]Na_2O$ (s, 298 K) + $x$SrO (s, 298 K) + $[(1-x)/2]Nb_2O_5$ (s, 298 K) + $x TiO_2$ (s, 298 K) → $Na_{1-x}Sr_xNb_{1-x}Ti_xO_3$ (s, 298 K) | (15) | $\Delta H^\circ_{f,ox}$ |
| $(1-x)$Na (s, 298 K) + $x$Sr (s, 298 K) + $(1-x)$Nb (s, 298 K) + $x$Ti (s, 298 K) + $(3/2)O_2$ (g, 298 K) → $Na_{1-x}Sr_xNb_{1-x}Ti_xO_3$ (s, 298 K)<br>$\Delta H^\circ_{f,el} = \Sigma \Delta H_i$ ($i = 11-14$) + $\Delta H^\circ_{f,ox}$ | (16) | |

exhibiting such an inverse relation between framework distortion and thermodynamic stability.

The opposite trend of $\Delta H^\circ_{f,ox}$ as a function of $(1 - t)$ prompts us to relate the stability with other structural parameter(s). A major feature of this solid solution series is that it is a mixture of charge types, the I−V perovskite $NaNbO_3$ and the II−IV type $SrTiO_3$. $Na_2O$ is a more basic oxide than SrO, and, for aluminates and silicates, for example, the sodium series have more exothermic heats of formation than the strontium series.[41] As demonstrated in numerous silicate systems including crystalline phases, glasses, and melts,[42] the energetic relations in $ABO_3$ perovskites may be explained by the dominance of acid−base chemistry in phase stability. Specifically, for oxide perovskites $ABO_3$ ($A = A^+, A^{2+}, A^{3+}$; $B = B^{5+}, B^{4+}, B^{3+}$), the most stable compounds form when the most basic binary A oxides combine with the most acidic B oxides

$$A_2O \text{ (or } 2AO \text{ or } A_2O_3) + B_2O_5 \text{ (}2BO_2 \text{ or } B_2O_3) = 2ABO_3 \quad (17)$$

since these reactions result in the most complete transfer of oxygen ions from the base to the acid oxides. The oxide basicity/acidity can be measured in terms of ionic potential of the metal cation, $z/r$, where $z$ is the formal charge and $r$ the ionic radius. The larger the $z/r$ of the cation, the less basic or the more acidic its oxide. To express the stability of $ABO_3$ perovskites, we define a parameter we call stability index ($s$) that equals the $z/r$ ratio between B and A cations:

$$s = (z/r)_B/(z/r)_A \quad (18)$$

For mixed-cation perovskites such as $Na_{1-x}Sr_xNb_{1-x}Ti_xO_3$, $(z/r)_A$ and $(z/r)_B$ are the averaged $z/r$ values of multiple A and B cations, respectively. Since the B oxide acts as the acid and A oxide the base, the larger the $s$, the more stable the perovskite. As the substitution, $Na^+ + Nb^{5+} \rightarrow Sr^{2+} + Ti^{4+}$, increases, $(z/r)_A$ increases; i.e., the basicity of A oxide decreases, whereas $(z/r)_B$ and thus the acidity of B oxide decreases. Therefore, the stability index $s$ becomes smaller, consistent with the less exothermic $\Delta H^\circ_{f,ox}$ with increasing Sr+Ti.

Figure 5 plots the formation enthalpies ($\Delta H^\circ_{f,ox}$) of $Na_{1-x}Sr_xNb_{1-x}Ti_xO_3$, together with those of other perovskites, including the two oxygen-deficient series exhibiting an inverse relation between $(1 - t)$ and $\Delta H^\circ_{f,ox}$,[39,40,43,44] as a function of $s$. With increasing $s$, $\Delta H^\circ_{f,ox}$ becomes more exothermic, and, further, the slope of the variation decreases

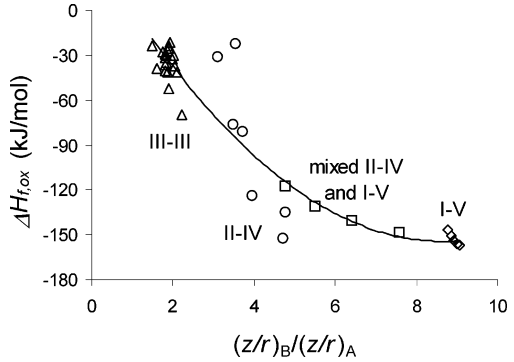


**Figure 5.** Variation of the enthalpies of formation of $ABO_3$ perovskites from the oxides as a function of $(z/r)_B/(z/r)_A$. Triangles represent $\Delta H_{f,ox}$ data for the charge type III−III, circles for II−IV, diamonds for I−V, and squares for the mixed II−IV and I−V type. The trend line is a polynomial fit to all the data.

from the charge type III−III to I−V. While the data for the III−III, I−V, and mixed II−IV and I−V perovskites fall well on the trend, those for the II−IV type somewhat deviate from the fitted line. Part of the reason for this deviation may be that the $\Delta H^\circ_{f,ox}$ data of the II−IV perovskites were measured at 1068 K, rather than the standard 298 K. Given the large difference in temperature, the assumption that the $\Delta H^\circ_{f,ox}$ (and $\Delta C_p$) values are temperature-independent may not be adequate.[44] However, the $\Delta C_p$ difference is not likely the only factor responsible for the scatter of the data, and to reveal other factors, more $\Delta H^\circ_{f,ox}$ data, especially those for the mixed III−III and II−IV perovskite type, would be needed.

**Enthalpies of Morphotropic Transitions.** As described above, with increasing Sr+Ti content, $Na_{1-x}Sr_xNb_{1-x}Ti_xO_3$ changes structure from the orthorhombic to tetragonal and then to cubic. However, the $\Delta H^\circ_{f,ox}$ varies with $x$ in a nearly linear fashion across the series (Figure 4A). This behavior implies that the enthalpies of these morphotropic transitions are small and are probably within the certainty of our calorimetric measurements.

As seen in other systems such as stuffed derivatives of quartz, $Li_{1-x}Al_{1-x}Si_{1+x}O_4$,[45] the compositionally induced transitions in $Na_{1-x}Sr_xNb_{1-x}Ti_xO_3$ are likely to be similar in character to those of individual phases with changing temperature. Thus, the magnitudes for the enthalpies of these two kinds of transitions ($\Delta H_{tran}$) should also be similar. On heating, $NaNbO_3$ perovskite undergoes a sequence of displacive transitions, largely via $[NbO_6]$ octahedral tilting, and eventually transforms to the cubic structure at ~914 K. The transition sequence is rather complex and may depend on the thermal history of samples.[33] Even after more than 40 years investigation, data concerning new $NaNbO_3$ phases at high temperatures or re-examination of known phases continue to appear.[33] Nevertheless, as the transitions mainly involve in rotation of $[NbO_6]$ octahedra, rather than breakage of the chemical bonds such as Nb−O, the enthalpies for these transitions are all small; their total is only less than 1 kJ/mol. Tennery and Hang reported four transitions whose

(35) Robie, R. A.; Hemingway, B. S. *Thermodynamic Properties of Minerals and Related Substances at 298.15 K and 1 Bar (105 Pascals) Pressure and at Higher Temperatures*; Geological Survey Bulletin No. 2131; U.S. Government Printing Office: Washington, DC, 1995.
(36) Chase, M. W. *NIST-JANAF Thermochemical Tables*; Journal of Physical and Chemical Reference Data, No. 9, ACS/AIP/NIST, 1998.
(37) Cheng, J.; Navrotsky, A. *J. Solid State Chem.* **2004**, *177*, 126.
(38) Navrotsky, A. In *Fundamental Physics of Ferroelectrics 2000: Aspen Center for Physics Workshop*; Cohen, R. E., Ed.; American Institute of Physics: Woodbury, NY, 2000, pp 288−296.
(39) Xu, H.; Su, Y.; Balmer, M. L.; Navrotsky, A. *Chem. Mater.* **2003**, *15*, 1872.
(40) Cheng, J.; Navrotsky, A. *J. Solid State Chem.* **2004**, *177*, 126.
(41) Roy, B. N.; Navrotsky, A. *J. Am. Ceram. Soc.* **1984**, 67, 606.
(42) Navrotsky, A. *Am. Mineral.* **1994**, *79*, 589.
(43) Takayama-Muromachi, E.; Navrotsky, A. *J. Solid State Chem.* **1988**, *72*, 244.
(44) Cheng, J.; Navrotsky, A. *J. Mater. Res.* **2003**, *18*, 2501.
(45) Xu, H.; Heaney, P. J.; Beall, G. H. *Am. Mineral.* **2000**, *85*, 971.

enthalpies were measurable by DSC, and the total value is 0.869 kJ/mol.[46] More recently, Pozdnyakova et al. reported a new transition at 600 K using DSC, and the total enthalpy for their measured five transitions is 0.42 kJ/mol.[33] Our own DSC measurement of $NaNbO_3$ gave a total heat of transitions of 0.56 kJ/mol. Further, DSC runs of the intermediate $Na_{1-x}Sr_xNb_{1-x}Ti_xO_3$ phases did not detect any transitions, indicating that their total $\Delta H_{tran}$ is even smaller than that of $NaNbO_3$. Since $Na_{1-x}Sr_xNb_{1-x}Ti_xO_3$ evolves toward the cubic structure with increasing Sr+Ti content, which is analogous to the structural evolution of $NaNbO_3$ on heating, the enthalpies for the morphotropic transitions are expected to be similar in order. These small magnitudes of enthalpies are essentially within the error of our calorimetric measurement, accounting for the linear relation between $\Delta H^\circ_{f,ox}$ and $x$ shown in Figure 4A.

In analogy to the thermally induced $NaNbO_3$ transitions, the morphotropic transitions in $Na_{1-x}Sr_xNb_{1-x}Ti_xO_3$ occur mainly via tilting of $[Nb/TiO_6]$ octahedra with increasing Sr+Ti content. This framework distortion results in evolution of the structure toward the cubic; i.e., the tolerance factor $t$ becomes closer to unity. However, since the enthalpies of the morphotropic transitions are small, structural distortions, expressed by $(1 - t)$, have insignificant effect on perovskite stability. Thus, the positive relation between $\Delta H^\circ_{f,ox}$ and $(1 - t)$ in most perovskite systems is likely not a reflection of their close correlation per se, as also evidenced by existence of the opposite $\Delta H^\circ_{f,ox} - (1 - t)$ trend in some systems. Calorimetric studies of perovskite solid solutions with the same degree of distortion (such as the cubic $KTaO_3$−$SrTiO_3$ system, $t \approx 1$) would provide additional evidence for the $\Delta H^\circ_{f,ox} - (1 - t)$ noncorrelation. Our proposed stability index ($s$), $(z/r)_B/(z/r)_A$, appears to correlate with $\Delta H^\circ_{f,ox}$ for all the perovskite systems whose formation enthalpies are available. This correlation is consistent with the dominance of the acid−base chemistry in phase stability, as seen in many other systems such as framework aluminosilicates in crystalline, glassy, and melt forms.

(46) Tennery, V. J.; Hang, K. W. *J. Am. Ceram. Soc.* **1968**, *51*, 469.

## Conclusions

A series of perovskite solid solutions along the $NaNbO_3$−$SrTiO_3$ join has been prepared using high-temperature sold-state synthesis. As Si+Ti content increases, the structure changes from the orthorhombic to tetragonal and to cubic. The enthalpy of formation $\Delta H^\circ_{f,ox}$ becomes less exothermic with increasing Sr+Ti content, suggesting a destabilization effect of the $Na^+ + Nb^{5+} \rightarrow Sr^{2+} + Ti^{4+}$ substitution on the perovskite structure with respect to the constituent oxides. This behavior can be interpreted as the dominance of the acid−base chemistry, expressed by $(z/r)_B/(z/r)_A$, on phase stability, which is also applicable to other perovskite systems. The linear variation of $\Delta H^\circ_{f,ox}$ with composition implies that the enthalpies for the morphotropic transitions are small.

**Acknowledgment.** This work was supported by the U.S. Department of Energy (DOE) Environmental Management Science Program (EMSP). Sample synthesis was conducted at the Environmental Molecular Sciences Laboratory, a national scientific user facility sponsored by the DOE Office of Biological and Environmental Research and located at the Pacific Northwest National Laboratory (PNNL). PNNL is operated for DOE by the Battelle Memorial Institute. We thank two anonymous reviewers for helpful comments and J. Cheng for help in compiling the calorimetric data for some perovskite systems.

CM047785I